coordination to the N7 or N1 atom of the adenine base in SAH agrees with the high kinetic affinity of Pt for the sulfur atom.[9,10] It is therefore not unlikely that significant amounts of platinum antitumor compounds will bind to sulfur-containing biomolecules. In fact *cis*-Pt is known to bind to plasma proteins and glutathione, and methionine-containing Pt(II) metabolites have been isolated from the urine of patients receiving *cis*-Pt.[24,25]

Given the absence of any binding to the adenosine unit, the Pt-coordination chemistry of SAH can now be reduced to that of a modified methionine molecule, under the assumption that the $Pt(dien)^{2+}$ coordination to the homocysteine is not sterically affected by the adenosine unit. The coordination chemistry of *cis*-Pt to methionine has recently been described by Appleton et al.[10] They also reported a high affinity for and an initial binding at the thioether sulfur. The subsequent chelating steps resulted in both *cis*-$[Pt(NH_3)_2$(met-*S*,*N*)$]^+$ and *cis*-$[Pt(NH_3)_2$(met-*S*,*O*)$]^{2+}$.[10] The formation of this six-membered chelate ring in *cis*-$[Pt(NH_3)_2$(met-*S*,*N*)$]^+$ already indicates that the amino group can be located in close proximity to the platinum, which in our case is a requirement for isomerization of **1** → **2**. Therefore a pentacoordinated transition state $[Pt(dien)SAH\text{-}S,N]^+$ is likely to occur.

SAH and analogues with modifications at the sugar moiety, at the amino acid residue, or at the purine ring are known to be potent inhibitors of biological methylation reactions catalyzed by *S*-adenosylmethionine-dependent methyltransferases.[26] This points to the possibility that compounds inhibiting these reactions can be pharmacologically active. The three metal complexes of SAH, described above, exemplify a complete new area of analogues of this compound. Therefore studies of the inhibition of this class of enzymes by these three Pt complexes may be worthwhile.

The first three metal complexes of SAH have been described in the present study. The results show that SAH, when reacting with Pt compounds, has a pronounced kinetic preference for the thioether linkage. The initially formed product isomerizes at pH > 7 to yield a thermodynamically favored product in which $Pt(dien)^{2+}$ is coordinated to the NH_2 group. This process can be reversed at pH < 5. The high reactivity of the Pt-S methionine bond toward nucleophiles is confirmed by its reaction with Na(ddtc). Ongoing studies are dealing with the coordination chemistry of [PtCl(dien)]Cl with synthetic *S*-guanosyl-L-homocysteine. In that case the reactivity of the sulfur atom can be directly studied and compared with the reactivity of N7 of the very reactive guanine.

Acknowledgment. This study was supported in part by the Netherlands foundation of Chemical Research (SON) with financial aid from the Netherlands Organization for the Advancement of Research (NWO), through Grant 333-17. Dr G. W. Canters is thanked for a careful reading of the manuscript and for many useful suggestions. We are indebted to Johnson Matthey Chemicals Ltd (Reading, England) for their generous loan of K_2PtCl_4. We acknowledge EC support (Grant No. ST2J-0462-C) allowing regular scientific exchange with the group of Prof. Dr. J. C. Chottard.

(24) Sternson, L. A.; Repta, A. J.; Shih, H.; Himmelstein, K. J.; Patton, T. F. In *Platinum Coordination Complexes in Chemotherapy*; Hacker, M. P., Douple, E. B., Krakoff, I. H., Eds.; Nijhoff: Boston, MA, 1984; pp 126-137.
(25) Berners-Price, S. J.; Kuchel, P. W. *Proc. Int. Conf. Coord. Chem.* **1989** *27*, T1.
(26) Ueland, P. M. *Pharmacol. Rev.* **1982**, *34*, 223-253.

Contribution from the Institut für Physikalische und Theoretische Chemie and Institut für Anorganische Chemie, Universität Regensburg, D-8400 Regensburg, FRG

Spectroscopic Studies of Cyclometalated Platinum(II) Complexes: Superposition of Two Different Spectroscopic Species in the Electronic Spectra of a Single Crystal of [Pt(bpm)$(CN)_2$] (bpm = 2,2'-Bipyrimidine)

Josef Biedermann,[†] Günter Gliemann,*[,†] Ulrich Klement,[‡] Klaus-Jürgen Range,*[,‡] and Manfred Zabel[‡]

Received August 28, 1989

The influence of temperature ($1.9 \le T \le 80$ K) and applied magnetic fields ($0 \le H \le 6$ T) on the optical properties of a single crystal of [Pt(bpm)$(CN)_2$] (bpm = 2,2'-bipyrimidine) is reported. These properties are due to two different kinds of chains (α and β) in the crystal. Chain α consists of quasi-isolated complexes with alternating Pt-Pt distances of 4.178 and 3.438 Å; chain β has a dimeric structure with Pt-Pt distances of 4.581 and 3.269 Å. At $T = 1.9$ K a luminescence exhibiting a sharp-line structure in the high-energy range and a broad weakly structured band in the low-energy range has been observed. The emission indicates a superposition of the electronic transitions in the α and β chains. When a magnetic field $\mathbf{H} \| \mathbf{a}$ is raised from $H = 0$ to 6 T, the intensity of the $\mathbf{E} \| \mathbf{a}$ polarized fine-structure lines increases by a factor of ~70. An applied magnetic field $\mathbf{H} \perp \mathbf{a}$ provides an increase of the $\mathbf{E} \perp \mathbf{a}$ and $\mathbf{E} \| \mathbf{a}$ polarized dimer emission by factors of 5 and 4, respectively. Both effects are explained by a magnetic field induced mixing of the lowest excited state with higher states. Crystallographic data for [Pt(bpm)$(CN)_2$]: triclinic, space group $P\bar{1}$, $a = 7.261$ (1) Å, $b = 10.828$ (1) Å, $c = 14.387$ (1) Å, $\alpha = 88.54$ (1)°, $\beta = 82.78$ (1)°, $\gamma = 74.07$ (1)°, $V = 1072.34$ Å^3, $Z = 4$, $D_x = 2.51$ g·cm^{-3}, μ(Cu Kα) = 249.0 cm^{-1}, $R = 0.025$ and $R_w = 0.033$ for 344 variables and 4411 reflections with $I > 3\sigma(I)$.

Introduction

During recent years, several efforts have been made to understand the photochemistry, photophysics, and electrochemistry of cyclometalated transition-metal complexes and related compounds.[1-7] Several of these systems can be employed as light-absorption sensitizers (LAS) and/or as light-emission sensitizers (LES) for the interconversion between light energy and chemical energy. Depending on the central ion and the ligands, the energetically lowest excited states of these systems were assigned to metal-centered (LF) states, ligand-centered (LC) states, or metal-to-ligand charge-transfer (MLCT) states.[8-15] Sometimes merely a variation of the solvent changes the type of the lowest

[†] Institut für Physikalische und Theoretische Chemie.
[‡] Institut für Anorganische Chemie.

(1) Ohsawa, Y.; Sprouse, S.; King, K. A.; DeArmond, M. K.; Hank, K. W.; Watts, R. J. *J. Phys. Chem.* **1987**, *91*, 1047.
(2) Maestri, M.; Sandrini, D.; Balzani, V.; Maeder, U.; von Zelewsky, A. *Inorg. Chem.* **1987**, *26*, 1323.
(3) Maestri, M.; Sandrini, D.; Balzani, V.; von Zelewsky, A.; Jolliet, P. *Helv. Chim. Acta* **1988**, *134*, 71.
(4) Maestri, M.; Sandrini, D.; Balzani, V.; Chassot, L.; Jolliet, P.; von Zelewsky, A. *Chem. Phys. Lett.* **1985**, *122*, 375.
(5) Bonafede, S.; Ciano, M.; Bolletta, F.; Balzani, V.; Chassot, L.; von Zelewsky, A. *J. Phys. Chem.* **1986**, *90*, 3836.
(6) Chassot, L.; von Zelewsky, A. *Inorg. Chem.* **1987**, *26*, 2814.
(7) Cornioley-Deuschel, C.; von Zelewsky, A. *Inorg. Chem.* **1987**, *26*, 3354.
(8) Demas, J. N. *J. Chem. Educ.* **1983**, *60*, 803.

0020-1669/90/1329-1884$02.50/0

excited state.[16,17] Most of the experiments and assignments mentioned above are restricted to solution and/or glasses. Relatively little information is available on the optical properties of the crystals. The compound $[Pt(bpm)(CN)_2]$ sets an example that relatively small variations of the crystal structure entail distinctly different optical features.

Depending on the conditions of crystallization, the complex molecules of $[Pt(bpm)(CN)_2]$ form crystals of different structures. As shown recently, the compounds $[Pt(bpm)(CN)_2]\cdot H_2O$ and $[Pt(bpm)(CN)_2]\cdot DMF$ crystallize according to the monoclinic space groups $P2_1/c$ and $P2_1/m$, respectively.[18,19] In both structures the $[Pt(bpm)(CN)_2]$ units are stacked, yielding mutually parallel columns. In a single crystal of $[Pt(bpm)(CN)_2]\cdot H_2O$ the Pt atoms are arranged on zigzag chains with alternating Pt–Pt distances r = 3.435 and 4.315 Å, whereas in $[Pt(bpm)(CN)_2]\cdot DMF$ the intrachain Pt–Pt distances are equidistant with a smaller r value (r = 3.284 Å). These structural variations result in fundamentally different optical properties. Both the optical absorption and the emission of $[Pt(bpm)(CN)_2]\cdot H_2O$ are typical for a system of oriented uncoupled $[Pt(bpm)(CN)_2]$ units.[18] A single crystal of $[Pt(bpm)(CN)_2]\cdot DMF$, however, yields absorption and emission spectra that show characteristic solid-state properties, indicating a distinct intercomplex coupling and a band structure of the electronic states relevant to the optical behavior.[19] Thus, $[Pt(bpm)(CN)_2]\cdot DMF$ is very similar to the crystalline tetracyanoplatinates(II).[20,21] This resemblance applies also to the effects of magnetic fields on the energy, the intensity, and the lifetime of the emission.[22,23]

$[Pt(bpm)(CN)_2]$ dissolved in DMSO forms crystals whose habitus is obviously dissimilar from that of $[Pt(bpm)(CN)_2]\cdot H_2O$ and $[Pt(bpm)(CN)_2]\cdot DMF$. The optical properties also differ distinctly. These observations suggest that a single crystal of $[Pt(bpm)(CN)_2]$ grown from a DMSO solution has a structure that differs appreciably from that of the other two crystalline systems. The purpose of this paper is to describe the crystal structure of $[Pt(bpm)(CN)_2]$ (from DMSO solution) and to report the polarized absorption and emission. Finally, an energy level system of the electronic states will be outlined, which supplies an interpretation of optical properties on the basis of the determined crystal structure.

Experimental Section

Single crystals of $[Pt(bpm)(CN)_2]$ have been grown by slow evaporation of a solution of $[Pt(bpm)(CN)_2]\cdot H_2O$ (cf. ref 24) in 100 mL of DMSO at 30 °C. The yellow needle-shaped crystals (size ~ 1 × 0.3 × 0.3 mm³) are stable in humid air.

The apparatus used for the spectroscopic measurements at different temperatures and under applied magnetic fields have been described in refs 21 and 23.

A single crystal of $[Pt(bpm)(CN)_2]$ (approximate dimensions 0.08 × 0.06 × 0.18 mm³) was used for data collection on an Enraf-Nonius CAD-4 diffractometer (CuKα, λ = 1.5418 Å, graphite monochromator in incident beam). The lattice constants have been refined from 2θ values of 25 reflections in the range $16.1 < \theta < 25.1°$. Intensities were measured for $2 \le \theta \le 75°$ in an ω–2θ scan technique, scan width $(0.6 + 0.14 \tan\theta)°$. An experimental correction of the serious absorption effects was applied, based on ψ-scans; transmission factors varied between 0.68 and 1.0. Three standard reflections indicated an intensity loss of 1.1% throughout data collection. Merging of the 8813 intensities ($(\sin\theta_{max})/\lambda = 0.62$; $-9 \le h \le 9$, $-13 \le k \le 13$, $-18 \le l \le 18$) gave 4411 unique reflections with $I > 3\sigma(I)$ (R_{int} = 0.011), which were considered as observed and used for all calculations (program systems SHELX-86 and SDP3.0, Enraf-Nonius).

The structure was solved by Patterson and direct methods (program SHELX-86), followed by difference Fourier syntheses. An $N(Z)$ test suggested a centric structure, and the space group $P\bar{1}$ was selected and later proved to be correct by the successful refinement.

In full-matrix least-squares refinement $|F|$ magnitudes were used to refine atomic coordinates for all atoms (including hydrogen), and anisotropic temperature factors were used for the non-hydrogen atoms and an exctinction parameter. Final R = 0.025, final R_w = 0.033, $w = 4I/(\sigma^2(I) + 0.0016I^2)$, Δ_{max}/σ for the non-hydrogen atoms was <0.01 in the final refinement cycle, 344 parameters were used, and S = 1.1. Maximum features in the final $\Delta\rho$ map: +1.1, −1.3 e A^{-3}.

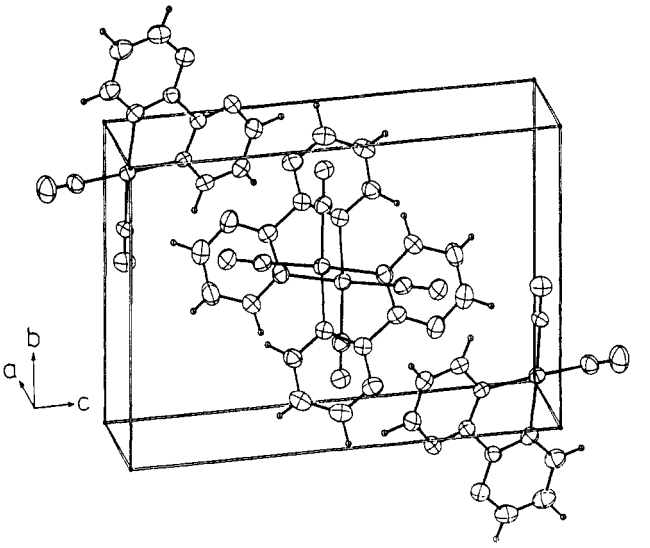

Figure 1. ORTEP plot of the complex $[Pt(bpm)(CN)_2]$ (bpm = 2,2′-bipyrimidine) in the unit cell of $[Pt(bpm)(CN)_2]$.

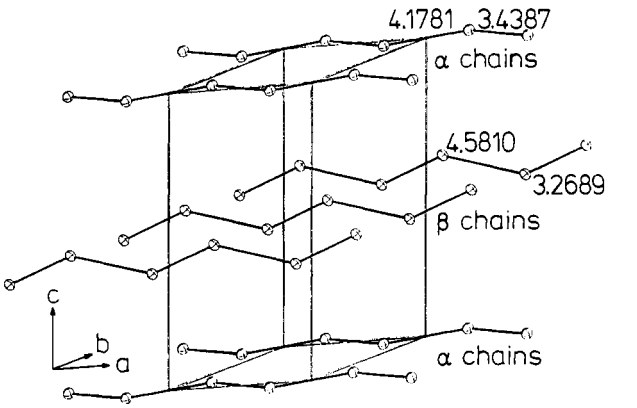

Figure 2. Chain structure formed by the platinum atoms in a single crystal of $[Pt(bpm)(CN)_2]$.

Table I. Crystal Data for $[Pt(bpm)(CN)_2]$ (bpm = 2,2′-Bipyrimidine)

M_r	405.29	V, Å^3	1072.34
space group	$P\bar{1}$	Z	4
a, Å	7.216 (1)	μ(Cu Kα), cm^{-1}	249.0
b, Å	10.828 (1)	T, K	298
c, Å	14.387 (1)	R_w^{iso}	0.056
α, deg	88.54 (1)	R^{aniso}	0.025
β, deg	82.78 (1)	R_w^{aniso}	0.033
γ, deg	74.07 (1)		

(9) DeArmond, M. K. *Coord. Chem. Rev.* **1981**, *36*, 325.
(10) Kalyanasundaram, K. *Coord. Chem. Rev.* **1982**, *46*, 159.
(11) Watts, R. J. *J. Chem. Educ.* **1983**, *60*, 834.
(12) Jamieson, M. A.; Serpone, N.; Hoffmann, M. Z. *Coord. Chem. Rev.* **1981**, *39*, 121.
(13) Serpone, N.; Hoffmann, M. Z. *J. Chem. Educ.* **1983**, *60*, 853.
(14) Juris, A.; Barigelletti, F.; Balzani, V.; von Zelewsky, A. *Inorg. Chem.* **1985**, *24*, 202.
(15) Balzani, V.; Bolletta, F.; Gandolfi, M. T.; Maestri, M. *Top. Curr. Chem.* **1978**, *75*, 1.
(16) Watts, R. J.; Crosby, G. A.; Sansegret, J. L. *Inorg. Chem.* **1972**, *11*, 1474.
(17) Watts, R. J.; Crosby, G. A. *Chem. Phys. Lett.* **1972**, *13*, 619.
(18) Biedermann, J.; Gliemann, G.; Klement, U.; Range, K.-J.; Zabel, M. *Inorg. Chim. Acta*, in press.
(19) Biedermann, J.; Gliemann, G.; Klement, U.; Range, K.-J.; Zabel, M. *Inorg. Chim. Acta*, in press.
(20) Gliemann, G.; Yersin, H. *Struct. Bonding* **1985**, *62*, 87.
(21) Tuszynski, W.; Gliemann, G. *Ber. Bunsenges. Phys. Chem.* **1985**, *89*, 940.
(22) Gliemann, G. *Comments Inorg. Chem.* **1986**, *5*, 263.
(23) Hidvegi, I.; von Ammon, W.; Gliemann, G. *J. Chem. Phys.* **1982**, *76*, 4361; **1984**, *80*, 2837.
(24) Kiernan, P. M.; Ludi, A. *J. Chem. Soc., Dalton Trans.* **1978**, 1127.

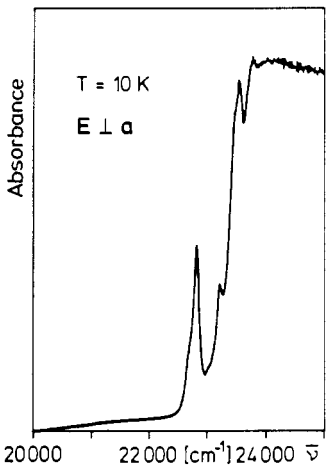

Figure 3. **E⊥a** polarized absorption spectrum of a single crystal of [Pt(bpm)(CN)$_2$] at T = 10 K. Thickness of the crystal is about 30 μm.

Results

Structure. [Pt(bpm)(CN)$_2$] crystallizes in the triclinic space group $P\bar{1}$. The unit cell contains four complex molecules as shown in Figure 1. In Table I the cell parameters are summarized. The complex molecule is isomorphous with those in single crystals of [Pt(bpm)(CN)$_2$]·H$_2$O[18] and [Pt(bpm)(CN)$_2$]·DMF.[19] The symmetry of the platinum atom and its surroundings corresponds to the point group C_{2v} (double group C_{2v}'). Two types, α and β, of mutually parallel zigzag chains formed by stacking of the complexes along the crystallographic a axis (needle axis) are observed. Figure 2 displays the positions of the platinum atoms. A chain of type α (type β) has the following structure: alternating Pt–Pt distances of r = 4.178 and 3.438 Å (4.581 and 3.269 Å), respectively; the inclination of the complex planes to the crystallographic b,c plane is ~10° (22°).

Spectroscopy. The **E⊥a** polarized absorption spectrum of a single crystal of [Pt(bpm)(CN)$_2$] (thickness ~30 μm) at T = 10 K is shown in Figure 3. For a concentration value of c = 6.193 M^{-1}, the maximum of the absorption band A (at $\bar{\nu}$ = 22 800 cm^{-1}) has an extinction coefficient of $\epsilon_\perp \sim 75$ M^{-1} cm^{-1}. At $\bar{\nu} > 23\,500$ cm^{-1} the extinction of the absorption increases strongly. In the low-energy range at $20\,000 \lesssim \bar{\nu} \lesssim 22\,000$ cm^{-1} a very weak, unstructured absorption is indicated. The extinction coefficient of this absorption is lower by a factor of ≳100 than that of band A. By measurements at T = 1.9 K the low-energy edge of band A has been determined to be at $\bar{\nu} = 22\,696 \pm 1$ cm^{-1}. The **E∥a** polarized absorption spectrum exhibits the same structure and differs mainly by its extinction coefficient $\epsilon_\parallel$, which is larger by a factor of about 4.5 than $\epsilon_\perp$.

Figure 4a shows the **E∥a** polarized emission spectrum of a single crystal of [Pt(bpm)(CN)$_2$] at T = 1.9 K. The spectrum is composed of a highly structured part at $22\,700 \gtrsim \bar{\nu} \gtrsim 20\,500$ cm^{-1} and a weakly structured, broad band X (half-width $\Delta\bar{\nu}_{1/2} \sim 1900$ cm^{-1}) with the maximum at $\bar{\nu} \sim 19\,400$ cm^{-1}. The **E⊥a** polarized spectrum has a very similar structure. Whereas band X exhibits nearly the same intensity for **E⊥a** and **E∥a** polarization, for the corresponding integral intensities $I_\perp$ and $I_\parallel$ of the spectral range displaying the fine structure, a ratio of $I_\parallel/I_\perp \sim 3$ has been found. For more details, the high-energy sections of the polarized emission spectra are presented in Figure 5 on a larger scale. As can be seen, the **E⊥a** and **E∥a** polarized spectra differ not by the peak energies but only by the relative intensities of corresponding fine-structure lines. In the spectra, characteristic groups of lines showing very similar internal structures occur several times. They are labeled I–VI. An example is group I composed of the line of highest energy (at $\bar{\nu}$ = 22 696 cm^{-1} with a half-width of $\Delta\bar{\nu}_{1/2} \sim 10$ cm^{-1}) and the three peaks red-shifted by $\Delta\bar{\nu}$ = 31, 109, and 244 cm^{-1}, respectively. Beside these groups, there exist several other emission lines. An obvious example is the sharp line at $\bar{\nu}$ = 21 964 cm^{-1}, being marked by an asterisk in Figure 5.

The spectral section of the fine-structure lines and the broad band X show different dependences on temperature. At T = 5 K the fine-structure lines are drastically reduced with the exception of the line at $\bar{\nu}$ = 21 964 cm^{-1} (cf. Figure 4b). By further increase of the temperature to T = 30 K (80 K) the **E⊥a** (**E∥a**) polarized emission at $\bar{\nu} \gtrsim 20\,800$ cm^{-1} is almost extinguished. Between T = 1.9 and 80 K no energy shift of the lines at $\bar{\nu} \gtrsim 20\,800$ cm^{-1} has been observed. With increasing temperature the shoulder of band X at $\bar{\nu} \sim 19\,600$ cm^{-1} acquires intensity. At T = 15 K the intensity of this shoulder is increased by a factor of about 5 and

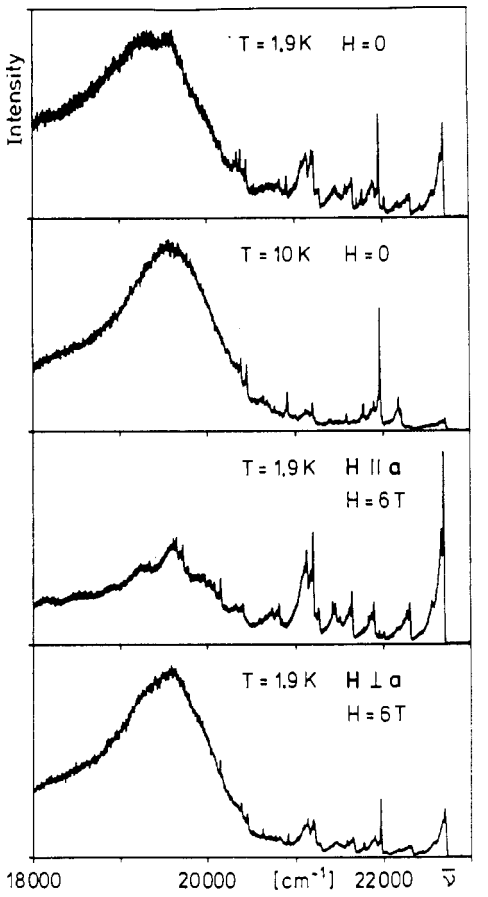

Figure 4. **E∥a** polarized emission spectra of a single crystal of [Pt(bpm)(CN)$_2$]: (a) T = 1.9 K, H = 0 T; (b) T = 10 K, H = 0 T; (c) T = 1.9 K, H = 6 T, **H∥a**; (d) T = 1.9 K, H = 6 T, **H⊥a**. λ_{exc} = 364 nm.

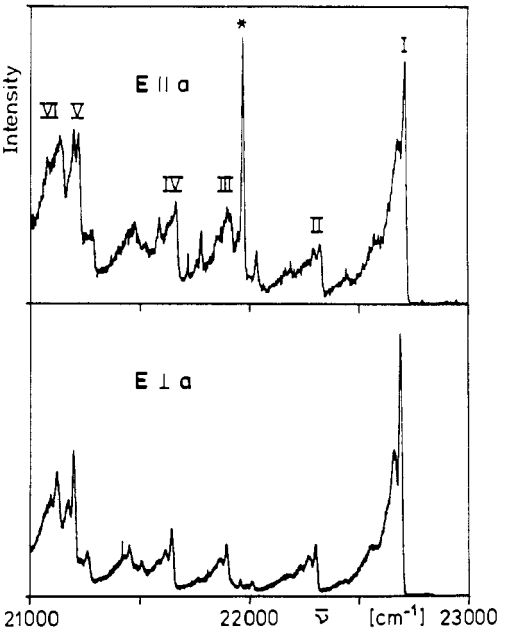

Figure 5. High-energy sections of the polarized emission spectra of a single crystal of [Pt(bpm)(CN)$_2$] at T = 1.9 K; λ_{exc} = 364 nm.

10 for $\mathbf{E}\parallel\mathbf{a}$ and $\mathbf{E}\perp\mathbf{a}$ polarization, respectively, and dominates the energy range of band X. Between $T = 15$ and 200 K the intensity of band X grows additionally by a factor of ~1.5. At higher temperatures the intensity is lowered, and at room temperature it reaches the 1.9 K value. Upon a temperature increase from $T = 1.9$ to 20 K the emission decay of band X is monoexponential and the emission lifetime is reduced from $\tau = 770$ to 60 μs. Between $T = 1.9$ and 100 K the emission lifetimes of the fine-structure lines were shorter than 60 μs (the lower detectivity limit of our present apparatus).

Homogeneous magnetic fields influence the emission of a single crystal of $[Pt(bpm)(CN)_2]$. The effect depends distinctly on the relative orientations of the field **H**, the polarization **E**, and the crystallographic axis *a*.

For $\mathbf{H}\parallel\mathbf{a}$, the $\mathbf{E}\perp\mathbf{a}$ polarized emission at $T = 1.9$ K shows no change of the fine-structure range and only a slight increase of the intensity of the shoulder of band X at $\bar{\nu} \sim 19\,600$ cm^{-1} (by a factor of ~1.5 at $H = 6$ T). The $\mathbf{E}\parallel\mathbf{a}$ polarized component, however, is strongly influenced by fields $\mathbf{H}\parallel\mathbf{a}$ at $T = 1.9$ K, as shown in Figure 4c. Between $H = 0$ and 6 T the intensity of all fine-structure lines is increased by a factor of ~25, but no spectral shifts have been observed. The magnetic field induced change of the intensity in the fine-structure range depends quadratically on the magnetic field strength H, $I_H - I_{H=0} \sim H^2$. Band X doubles its intensity with maximum at $\bar{\nu} \sim 19\,500$ cm^{-1}, and its structure becomes more pronounced, showing a progression of about $\Delta\bar{\nu} \sim 360$ cm^{-1}.

The fine-structure range is not influenced by magnetic fields $\mathbf{H}\perp\mathbf{a}$ at $H \leq 6$ T and $T = 1.9$ K, neither for $\mathbf{E}\parallel\mathbf{a}$ nor for $\mathbf{E}\perp\mathbf{a}$ polarization. The intensity of band X, however, is increased by factors of ~5 and ~4 for $\mathbf{E}\perp\mathbf{a}$ and $\mathbf{E}\parallel\mathbf{a}$ polarization, respectively, and the half-width is reduced from $\Delta\bar{\nu}_{1/2} = 1900$ to 1200 cm^{-1} when the field strength is raised from $H = 0$ to 6 T (cf. Figure 4d). This effect is due to the intensity increase of the shoulder at $\bar{\nu} \sim 19\,600$ cm^{-1}.

The emission lifetime of band X can be influenced by magnetic fields with $\mathbf{H}\perp\mathbf{a}$ but not with $\mathbf{H}\parallel\mathbf{a}$. Between $H = 0$ and 6 T the lifetime at $T = 1.9$ K is shortened from $\tau = 770$ to ~60 μs, independent of the polarization of the emitted light. For $\mathbf{E}\parallel\mathbf{a}$ and $\mathbf{E}\perp\mathbf{a}$ polarization $1/\tau_H - 1/\tau_{H=0}$ is a purely quadratic function of H.

Discussion

The observed properties of the polarized optical absorption and emission of a single crystal of $[Pt(bpm)(CN)_2]$ can be traced back to a superposition of the corresponding properties of the two types, α and β, of chains forming the crystal. As will be shown below, the absorption at $\bar{\nu} \geq 22\,696$ cm^{-1} and the emission at $20\,500 \lesssim \bar{\nu} \leq 22\,696$ cm^{-1} are due to the α chains, whereas the very weak absorption at $\bar{\nu} < 22\,696$ cm^{-1} and the broad emission band X belong to the β chains.

The shortest intrachain Pt–Pt distance in an α chain is $r_\alpha^{min} \sim 3.43$ Å. That value has been observed also for the shortest Pt–Pt distance in a single crystal of $[Pt(bpm)(CN)_2]\cdot H_2O$.[18] As for this system, the orbital overlap of neighboring complex molecules in an α chain is expected to be small, and, thus, an α chain behaves optically nearly as a system of oriented single complex molecules. As shown in ref 18, the HOMO and LUMO of a $[Pt(bpm)(CN)_2]$ molecule are hybrids $a_2(xy, \pi_{bpm})$ and $b_1(x, \pi^*_{CN}, \pi^*_{bpm})$, respectively. The representations a_2 and b_1 refer to C_{2v} symmetry; *xy* and *x* are abbreviations of the metal orbitals $5d_{xy}$ and $6p_x$, respectively. Electron interaction (and spin–orbit coupling) included the ground state and the lowest excited electronic states of the complex molecule and can be classified as $^1A_1(A_1')$, $^3B_2(A_1', A_2', B_1')$, and $^1B_2(B_2')$. The primed symbols label the spin–orbit components according to the double group C_{2v}'.

The absorption at $\bar{\nu} \geq 22\,696$ cm^{-1} can be assigned to the symmetry-allowed singlet–triplet transitions from the ground electronic state A_1' to the nearly degenerate exciton bands A_1' and B_1' and to corresponding vibrational satellites. The electronic transitions are $\mathbf{E}\perp\mathbf{x}$ and $\mathbf{E}\parallel\mathbf{x}$ polarized, respectively. Since both the HOMO and the LUMO have partly metal character, the relatively large values of the extinction coefficients can be understood. The observed polarization ratio of the absorption is partially conditioned by the inclination of the molecular *x* axis to the crystallographic *a* axis, and it yields for the extinction coefficients a ratio $\epsilon(A_1' \rightarrow A_1')/\epsilon(A_1' \rightarrow B_1')$ of about 0.2. Unlike a single crystal of $[Pt(bpm)(CN)_2]\cdot H_2O$, the crystals of the title compound show no indication of low-lying X-traps in the absorption spectrum.

The high-energy range of the emission of a single crystal of $[Pt(bpm)(CN)_2]$ at $T = 1.9$ K exhibits the same fine structure as the emission spectrum of a single crystal of $[Pt(bpm)(CN)_2]\cdot H_2O$ at $T = 15$ K, except for an energy shift of $\Delta\bar{\nu} = 124$ cm^{-1}, which may be due to a slightly different coupling of the complex molecules with their surroundings in both systems. For $[Pt(bpm)(CN)_2]\cdot H_2O$ at $T = 15$ K, the low-lying X-traps are thermally depleted and the emission is due to the radiative deactivation of the corresponding exciton bands. Thus, it can be concluded that a single crystal of $[Pt(bpm)(CN)_2]$ has no low-lying X-traps of perceptible concentration and the highly structured emission is owing to the emission from the exciton bands A_1' and B_1', belonging to the very weakly coupled complex molecules in the α chains. The progressions and the sidebands in the emission spectra at $\bar{\nu} \leq 22\,696$ cm^{-1} originate probably from a coupling of totally symmetric vibrations of the complex molecules and of phonons. From the intensity ratio $I_\parallel/I_\perp \sim 3$ and from the inclination angle of the *x* axes ($\phi \sim 10°$) it can be concluded that the exciton band A_1' is by about $\Delta\bar{\nu} \sim 2$ cm^{-1} lower in energy than the B_1' band. The magnetic field induced increase of the low-temperature emission with $\mathbf{E}\parallel\mathbf{a}$ polarization can be explained on the basis of perturbation theory.[22] A homogeneous magnetic field $\mathbf{H}\parallel\mathbf{a}$ reduces the symmetry of the system, and the triplet components A_1' and B_1' can mix. With increasing field strength the admixture of B_1' to the lowest excited state grows and dominates the emission.

Within a β chain the complex molecules form dimers with a Pt–Pt distance of $r_\beta^{min} \sim 3.269$ Å. Except for their mutual 180° rotation, the complex molecules of a dimer have face-to-face arrangement with the Pt–Pt axis (*x* axis) nearly perpendicular to the planes of the molecules. A comparable structure has been observed for a single crystal of $[Pt(bpm)(CN)_2]\cdot DMF$.[19] In this compound the $[Pt(bpm)(CN)_2]$ units are stacked equidistantly with a Pt–Pt value of ~3.284 Å and have also a face-to-face arrangement. The optical properties of a single crystal of $[Pt(bpm)(CN)_2]\cdot DMF$ could be traced back to the formation of electronic bands due to a relatively strong interaction of neighboring complex molecules. By this interaction the LUMO's $b_1(x, \pi^*_{CN}, \pi^*_{bpm})$ split and yield the conduction band. The splitting of the HOMO's $a_2(xy, \pi_{bpm})$ is distinctly smaller than that of the strongly overlapping metal states $5d_{x^2}$. Thus, these $a_1(x^2)$ states form the valence band whose upper edge has an energy higher than that of the above-mentioned a_2 band of the molecule HOMO's.

From Hückel's MO theory as a rough approximation, it follows that the resonance splitting for a dimer is only half as large as for a chain of equidistant complex molecules. That means the splitting of the two low-lying $a_1(x^2)$ states of the dimer $[Pt(bpm)(CN)_2]_2$ may be too small to yield the HOMO of the dimer. In this case the antibonding state, formed by the HOMO's $a_2(xy, \pi_{bpm})$ of the two single complex molecules, is the HOMO of the dimer. As will be shown below, this case is true for the β chains of the title compound.

For a correct description of the electronic states of the dimer $[Pt(bpm)(CN)_2]_2$ the point group C_{2h} (double group C_{2h}') of this system has to be taken into account. The HOMO's of the two complex molecules of the dimer yield as dimer states the bonding $a_u(xy, \pi_{bpm})$ and the antibonding $b^*_g(xy, \pi_{bpm})$, whereas the two molecule LUMO's form the two dimer states $a_g(x, \pi^*_{CN}, \pi^*_{bpm})$ and $b^*_u(x, \pi^*_{CN}, \pi^*_{bpm})$. b^*_g and a_g are the HOMO and LUMO, respectively, of the dimer. With regard to electron interaction (and spin–orbit coupling), the ground electronic state transforms according $^1A_g(A_g')$, and the low-energy excitation $b^*_g \rightarrow a_g$ yields the states $^3B_g(B_g', A_g', A_g')$ and $^1B_g(B_g')$, as shown schematically

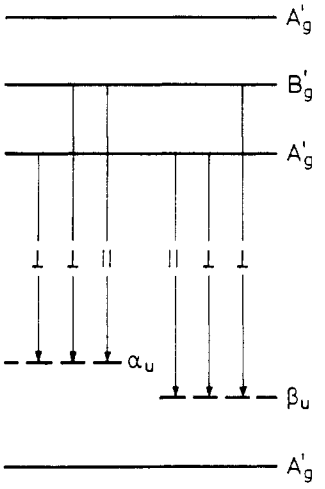

Figure 6. Energy level diagram for the electronic states of a β chain in a single crystal of $[Pt(bpm)(CN)_2]$.

in Figure 6. Electric dipole transitions between the ground state and these excited states are parity forbidden. By vibronic coupling with excited states of odd parity, the following polarized optical transitions $A_g' \leftrightarrow A_g'$, B_g' with vibrations of symmetry α_u and β_u are expected (cf. also Figure 6):

	A_g'	B_g'
A_g'	α_u:E‖y	α_u:E‖x or z
	β_u:E‖x or z	β_u:E‖y

The very weak absorption at $\bar{\nu} \sim 21\,000$ cm^{-1} can be assigned to a spin- and symmetry-forbidden transition from the ground electronic state A_g' to the triplet components of ^3B_g parentage.

The broad emission band X is due to the radiative deactivation of the lowest excited triplet components. Both the polarization properties of band X and its dependence on temperature and applied magnetic fields can be understood on the basis of the energy level scheme given in Figure 6. The energy order of the lowest excited electronic states and of the vibrational quanta have been chosen according to the experimental results, as will be shown below. The energy distance between the triplet components is expected to be on the order of several wavenumbers.

At $T = 1.9$ K only the lowest excited state A_g' is appreciably occupied. The vibronic transition $A_g' \rightarrow A_g' + \beta_u$ yields both an E‖x and an E⊥x emission, both of equal energy. These emissions correspond to the nonpolarized shoulder of band X at $\bar{\nu} \sim 19\,600$ cm^{-1}, whereas the transition $A_g' \rightarrow A_g' + \alpha_u$ is hidden below the vibrational structure at $\bar{\nu} < 19\,600$ cm^{-1}. With increasing temperature the state B_g' becomes thermally populated. The vibronic transition $B_g' \rightarrow A_g' + \beta_u$ is E⊥x polarized. It is composed of an E‖a and a more intense E⊥a component. Because of the admixture of the singlet $B_g'(^1B_g)$ to the triplet B_g' via spin–orbit coupling, the radiative deactivation rate for the transition $B_g' \rightarrow A_g' + \beta_u$ will be distinctly larger than that for the corresponding transition from the lowest excited state A_g'. That explains the temperature-induced increase of the emission intensity at $\bar{\nu} \sim 19\,600$ cm^{-1}. The small energy difference between A_g' and B_g' cannot be detected spectroscopically. The radiative rate of the process $B_g' \rightarrow A_g' + \alpha_u$ is obviously lower than that of the transition $B_g' \rightarrow A_g' + \beta_u$.

The β-chain emission can be influenced by homogeneous magnetic fields with H⊥x but not with H‖x. Fields with H‖x do not change the symmetry of the system. For the orientation H⊥x, however, the symmetry is reduced to C_i, and the states $A_g'(A_g')$ and $A_g'(B_g')$ can mix. As a consequence, the $A_g'(B_g')$ component of the lowest excited electronic state raises the radiative rate at low temperatures and an effect similar to that found with a temperature increase results. The slow intensity increase of the X band for H‖a is due to the effective H⊥x component.

Acknowledgment. This research was supported by the Deutsche Forschungsgemeinschaft and the Fonds der Chemischen Industrie.

Supplementary Material Available: Tables of positional parameters and bond distances and angles (4 pages). Ordering information is given on any current masthead page.

Contribution from the Institut de Chimie Physique, Ecole Polytechnique Fédérale, CH-1015 Lausanne, Switzerland

Photophysics and Photoredox Reactions of Ligand-Bridged Binuclear Polypyridyl Complexes of Ruthenium(II) and of Their Monomeric Analogues

K. Kalyanasundaram* and Md. K. Nazeeruddin

Received March 2, 1989

The influence of bridging ligand (BL), spectator ligand (LL), and solvent on the photophysical properties of the MLCT state has been assessed in a series of mono- and binuclear polypyridyl complexes of Ru(II); $\{[(LL)_2Ru]_n(BL)\}^{2n+}$ (n = 1, 2; BL = 2,2'-bipyrimidine (bpym), 2,3-bis(2-pyridyl)pyrazine (dpp); LL = a substituted 2,2'-bipyridine (bpy), 1,10-phenanthroline (phen)). A comparative study of the two series of complexes with dpp or bpym as the bridging ligand allows some of the reported anomalies in the behavior of the latter series of complexes to be explained. Features in the excited-state absorption spectra of the ligand-bridged binuclear complexes are also reported. Chemical and photochemical oxidation of the binuclear complexes from the (II,II) state to (II,III) and (III,III) states are examined. Complexes in the (III,III) state are unstable and rapidly cleave into monomeric components.

Introduction

Extensive photophysical and photochemical studies on the polypyridyl complexes of Ru(II) in the last 2 decades[1,2] have allowed development of quantitative descriptions of the excited-state dynamics and also practical applications of these complexes in areas such as photochemical conversion of solar energy. With the enormous success obtained with the mononuclear complexes, increasing attention is being focussed on polynuclear ("supramolecular") complexes.[3-7] Optical excitation of polynu-

(1) Juris, A.; Balzani, V.; Belser, P.; von Zelewsky, A. *Coord. Chem. Rev.* **1988**, *84*, 85.
(2) Kalyanasundaram, K. *Coord. Chem. Rev.* **1982**, *46*, 159.
(3) Balzani, V.; Sabbatini, N.; Scandola, F. *Chem. Rev.* **1987**, *86*, 319.
(4) Balzani, V., Ed. *Supramolecular Photochemistry*; NATO ASI Series C214; Reidel: Dordrecht, The Netherlands, 1987.

0020-1669/90/1329-1888$02.50/0